

Variable stars in the core of the globular cluster M3

Jay Strader^{1,2}, Henry O. Everitt^{1,3}, Stephen Danford⁴

¹Department of Physics, Duke University, Box 90305, Durham, NC 27708

²Department of Physics, Auburn University, Auburn, AL, 36830, stradm@auburn.edu (current address)

³U.S. Army Research Office, Box 12211, RTP, NC 27709, everitt@aro.arl.army.mil

⁴Department of Physics & Astronomy, University of North Carolina–Greensboro, P.O. Box 26170, Greensboro, NC, 27402, danford@uncg.edu

2 December 2024

ABSTRACT

We present the results of a survey for variable stars in the core of the globular cluster M3. Our findings include the discovery of twelve new variables, including a possible W Vir, and the first period determinations for thirteen previously known variables. Our results provide additional support for the feasibility of a large scale, systematic survey for variable stars in the cores of galactic globular clusters that would require only modest instruments.

Key words: stars: variables: other – globular clusters: general – globular clusters: individual: M3 – techniques: image processing

1 INTRODUCTION

M3 is the most variable-rich galactic globular cluster (Fig. 1), and the majority of these variable stars are RR Lyraes (RRLs). Although the outer portions of the cluster were long ago surveyed for variables (e.g. Bailey 1913; Sawyer 1973), the identification and classification of RRLs in the core has proven much more difficult. Many variables in the core, though identified as such, have poor or undetermined periods and light curves. The advent of image subtraction techniques for differential photometry, particularly the recent work of Alard (2000), has made systematic searches for RRLs in the cores of globular clusters with modest (i.e. ≤ 1 -m) instruments possible. Such studies will help to elucidate the radial distribution of the different classes of RRLs. In addition, the wide variety of pulsation behavior of RRLs serves as a testbed for theories of stellar evolution, and regular monitoring of possible period changes in RR Lyraes may help to shed light upon such phenomena as the Blazhko and Oosterhoff effects (Blahzko 1907; Oosterhoff 1939).

2 OBSERVATIONS AND REDUCTIONS

2.1 Observations

All images were taken at the Three College Observatory (TCO), located in Snow Camp, NC, between Durham and Greensboro. Built in 1981 and operated by the University of North Carolina-Greensboro, TCO houses a 0.81-m f/13.5 Ritchey-Chretien telescope. It is equipped with a 1024 \times 1024 Texas Instruments 215 charged-coupled display (CCD), binned to 512 \times 512. The pixel scale is 0.46'', with a 3'51'' \times 3'51'' field of view.

Observations were made on fifteen nights from March to July 2001. Seeing ranged from 1.5 to 2.0 arcsec. Images were taken in the *V* band, and exposure times were generally 160 s since longer exposures saturated the central part of the core. Eleven of the fifteen nights produced at least one image suitable for differential photometry. In total, 61 images were of sufficient quality to be used in subsequent analysis. All images were taken with the CCD set to the same field.

2.2 Reductions

The Image Reduction and Analysis Facility (IRAF) was used for the standard data reduction. All frames were trimmed, debiased, and flat-fielded using dome flats. Since all analysis was performed using only differential photometry, no standard stars were observed to calculate coefficients for magnitude transformation equations.

2.3 Image Subtraction

The reduced images were processed using the image subtraction method (ISM) of Alard and Lupton (1998), as implemented in the package ISIS 2.1, obtained through private communication with C. Alard. Five of the images with the best seeing were combined to serve as the reference frame. All images were registered to the reference frame, and then for each image, a third-order convolution kernel was formed. The convolved reference frame was then subtracted from each individual frame. Then, for each pixel, a time series of these residual fluxes was created. Data points more than three standard deviations from the median were removed from the time series to account for contaminating events, such as cosmic rays or severe atmospheric disturbances. The

median of this corrected set of data became a robust statistic for the variability of that pixel. The composite of all of these pixel statistics, essentially a stacked residual image, was denoted *var.fits*.

On *var.fits*, the only stars visible were variable stars—primarily RR Lyraes (Fig. 2). A routine was then run to search for objects in *var.fits*. To avoid missing variables in the crowded core, the detection limit was set to only one standard deviation, so that the program found all objects whose ‘brightness’ was more than 1σ above the local background. Any detections that were clearly false positives were then removed manually.

For each of the suspected variable stars, an unphased light curve was produced. The ISIS built-in routine for aperture photometry calculated the differential flux for each of the residual images. The aperture radius was six pixels.

3 ANALYSIS

3.1 Period Searching

To search for the periods of the suspected variables, Lomb-Scargle periodogram (Scargle 1982) and phase dispersion minimization (PDM) (Stellingwerf 1978) methods were used, as implemented in the R. Barbera’s AVE program¹. For each star, both methods were used to search for the best-fit period as described in this section. In nearly all cases, the resulting periods agreed to the fourth or fifth decimal place. When discrepancies existed, visual inspection of the resulting light curves was used to choose the period that minimized the scatter in the light curve.

Since the focus of the search was on RRLs, the period range 0.2–0.8 days was searched. In a few cases, when no accurate period could be found in that interval, the range was extended at both ends to allow for the rare possibility of a Cepheid or RGB star.

For the majority of the stars in the outer portions of the images, the PDM/periodogram (PDMP) analysis showed a single clear period and produced a relatively clean light curve when fit to the data. For those stars closer to the core, however, the PDMP analysis did not always suggest a single period. In these cases, periods corresponding to all of the respective PDMP extrema were tried, and the resulting light curves were compared. In many cases it was possible to eliminate other periods because they were incompatible with the type of the RRL, as indicated by the shape of the light curve. If these methods still left multiple possible periods, the candidate light curves were inspected visually to ascertain the most accurate period. For a small number of cases, no such determination could be made, and no period was assigned.

For a few stars, the noise in the light curve can be at least partially attributed to the presence of a nearby star (variable or not), whose light interferes with the signal from the variable star. These stars have been marked as ‘merged’ in Table 1.

¹ Version 2.51 may be found at <http://www.astrogea.org/soft/ave/aveint.htm>

3.2 Identification

After calculating preliminary periods for all of the detected variables in the images, RA/Dec coordinates were found for each star. To do this, 20 variables were identified using the finder charts in Carretta et al. (1998) [C98]. Each variable had its identity confirmed using rough period matching from values given in the same source. Since complete astrometry for all previously known variables is given in Bakos et al. (2000) [B00], it was possible to obtain accurate RA/Dec values for each of these known RRLs. The IRAF tasks *ccmap* and *wcsctran* were then used to compute transformation equations from physical (pixel) to world (RA/Dec) coordinates for the images, and thus assign RA/Dec coordinates to each variable star in the sample. Since the accuracy of the B00 astrometry was ≤ 0.2 arcsec, the process of matching variables in the sample to known RRLs was greatly facilitated.

For nearly all detected variables, the RA/Dec matches provided an accurate means of identifying RRLs in our sample. A second means of verification was period matching. For each variable, the period was taken from the most recent source available, which was usually CC01. If the star was not included in the CC01 sample, an older period determination could sometimes be found in catalogue of Clement et al. (2001) [C01], an updated version of (Sawyer 1973).

4 RESULTS

We identified 140 variable star candidates using the above procedures. Of these 140, 131 proved to be variable, and these are listed in Table 1. The new and published periods are compared, and comments are added where appropriate.

4.1 Error Analysis

The method used here calculates light curves using uncalibrated instrumental fluxes. This contrasts with most prior analyses of M3 RRL light curves which were plotted using standard apparent magnitudes. In this section, we address the self-consistency of this method and compare the results to published photometry of RRLs.

4.1.1 Self-Consistency

To test the sensitivity of the period searching method to variations in the data, two stars were selected at random, one with a very clean light curve and the other with a relatively noisy one. Five data points, equivalent to eight per cent of the total data set, were then randomly selected for each star and removed from the set of observations. The period searching algorithm was then run as previously discussed.

v77 was chosen as the star with the clean light curve. Period analysis on both the full and reduced data sets gave the same period, 0.459419 d. The resulting light curve is slightly better than that produced using the published value from CC01, 0.459350 d.

v214 was selected for its more scattered light curve. In this case, the best fit period changed from 0.539507 d to

0.539492 d. These are both close to the most recent published period, 0.539493 d, taken from CC01. A visual inspection of the light curves for our two derived periods show no significant differences.

These results imply that our method is fairly robust: a slight perturbation of the data set does not have a substantial impact on our derived periods to four decimal places.

4.1.2 Comparison with Published Periods

Another test of the accuracy of our method is how well it reproduces periods and light curves for well-studied stars. One difficulty is that we are studying primarily the inner core of M3, where the scatter in the data is inherently higher. However, many stars with previously measured periods were included in our field of view.

For example, many variable stars in the uncrowded outer portions of M3 were studied here and by CC01. For each of these variable stars, the light curves associated with the respective periods were compared by PDMP analysis and by visual inspection. In many cases the period search algorithm was used on an interval that contained the CC01 period and excluded ours to ascertain whether the CC01 period was a secondary extrema in the PDMP analysis of our data.

For each star studied by CC01 and included in our sample, we found that the period determined by our analysis gave a fit that matched or exceeded the fit obtained using the CC01 period. In the latter cases, though the CC01 period might have a larger number of decimal places, PDMP analysis and visual inspection suggested that our periods were a better match than the CC01 periods to our data. In total, we found that 70 stars had period differences of less than 0.001 d between our period and the CC01 period. Twenty-eight additional stars had period differences of 0.001 d or more.

Since M3 is an Oosterhoff I cluster, the expected period change rate (β) is relatively low—CC01 found that typically, $\beta < 1$ day Myr⁻¹. Thus, given that the CC01 periods were determined using 1992–1997 data, it seems unlikely that more than a few of these differences could be reasonably attributed to period changes.

For seven of these 28 stars (v41, v148, v165, v170, v201, v209, v226) our periods agree with the C98 or C01 periods to within 0.001 d. Nine of the remaining 21 stars are listed as “blends” by CC01. Their color index suggests the light of the variable star is mixed with that of a nearby non-variable star. Two additional stars merged with other RRLs (v122 with v229, v241 with v262). This merging may have led to a somewhat higher uncertainty in the period. For these eleven stars, we could not make an unambiguous determination as to which period gave a superior fit.

Seven of the remaining ten stars have noisy published light curves in CC01. Two of these stars (v193, v235) had coverage too poor in our data set to make a definite determination between our period and the CC01 period. For each of the other five stars, we plotted the light curves for both periods, and present them side by side for comparison in Figure 3. Visual inspection of these light curves indicates that our periods give superior results for each of these five stars. Though three of these five stars (v161, v175, v184)

have periods included in C01, neither our periods nor those of CC01 agree with the C01 periods to 0.001 d.

Only three of the original 28 stars with period discrepancies greater than 0.001 d have both clean published light curves in CC01 and clean light curves when phased with our periods. Further study of these variables (v149, v208, v219) is needed to determine the correct periods.

4.1.3 Accuracy

These consistency tests and the fact that the data spanned between 200–400 cycles of most variables led us to conclude that our measured periods were accurate to approximately 0.0001 d. In some cases our periods appear to be valid to at least 0.00001 d, and revised periods spanning many more cycles will be published in a future paper. Therefore, all of the measured period values in Table 1 are rounded to four decimal places. Published values are rounded to four places for comparison.

4.2 Notes on Individual Variables

Comments on some of the newly discovered, suspected, and previously known variable stars are given below. Light curves for the newly discovered variables, labeled S1–S12, are presented in Figure 4, unless no period could be determined. RR Lyrae types are identified using the descriptive nomenclature of C01, based on pulsation modes. In this system, RR0 and RR1 denote fundamental and first overtone pulsators, respectively, corresponding to Bailey types RRab and RRc. RR01 refers to double-mode stars pulsating in both the fundamental and first overtone frequencies, commonly called RRd stars.

v29: CC01 misidentifies this star as v155, an error present in a previous paper (Evstigneeva et al. 1994).

v122: Although the light curve produced by our period, 0.5165 d, is noisy, that given by CC01, .5060 d, does not fit the data. The discrepancy is likely due to the merging of v122 with v229 on the images.

v154: Because our data covers only 12 full cycles of this star, it is likely that our period, 15.43 d, is less accurate than that published in C01 (15.28 d), although our results do agree with C01 to the twelve period (\sim eight per cent) accuracy our data allows.

v224: This star does not appear to be variable, but a definite determination could not be made using our data set. It is identified as variable X38 in Kholopov (1977).

v250: There is no previous period determination for v250, for which there are two close candidate stars (Bakos et al. 2000) in the WF/PC Hubble Space Telescope images of Guhathakurta et al. (1994). The confusion due to the companion resulted in an inconclusive PDMP, with several possible periods. Visual inspection of the resulting light curves suggests a period of 0.5586 d.

v273: This star was identified as a long period variable by B00. Our analysis gives a period of 46.43 d, although this is poorly constrained because fewer than three cycles are covered by our observations. If this period is correct, the star could be a short period SR-type or a long period W Vir.

S1: This star has a large scatter in its light curve. Al-

though a period of 0.3868 d best fits our data, this is unusually short for an RR0. A possible alternate period is 0.6310 d.

S2: The light curve is very noisy, but apparently that of an RR1. There are no obvious period candidates besides 0.2980 d.

S3: The period 0.3965 d provides the best fit. There is little data around maximum, however.

S5: Though 0.5075 d falls outside the normal range for RR1 variables, the light curve most closely resembles that of an RR1 and gives a clean fit to the data. Such a classification is not unprecedented in M3—the RR1 star v70 has a CC01 period of 0.4861 d. However, more data is needed to confirm this assignment.

S7: Although the period 0.6090 d gives the best fit, the light curve is very noisy.

S8: No period in the normal RR Lyrae range (0.2 d - 0.8 d) fits our data. We find possible periods of 0.9883 d, 1.3267 d, and 4.0433 d, with the second of these producing the least scatter. The first two periods fall within the W Vir range, but since no magnitudes were calculated, we cannot confirm whether its period matches that predicted by the Population II Cepheid period-luminosity relationship. While it could be a star on the tip of the RGB, the best fit periods are far too short for the most common candidates (e.g. Mira, SR). Thus, until more observations are made, we label this a suspected W Vir, period 1.3267 d.

S9: Our analysis suggests that this may be a long period variable, possibly an SRa or SRb. No unambiguous period measurement was possible over the limited time baseline of 119 d.

S10: The period .4261 d is favored by our analysis; however, large scatter near the minimum and poor coverage make this value uncertain.

S11: While the best fit for our data, the period 0.4778 d nevertheless gives an extremely noisy RR0 light curve.

S12: This star is likely an RR0 variable, but no clear period could be found.

5 CONCLUSIONS

We have conducted a survey of variable stars in the core of the globular cluster M3. We discovered twelve new variable stars, which include ten RR Lyraes, one unidentified long period variable, and a suspected W Vir. For thirteen previously known variable stars, our period determinations are the first. Additionally, we have updated period data for dozens of other poorly studied stars in the core. The success of this study, due largely to the efficiency of the Alard ISM, should be taken as further evidence for the feasibility of a systematic large scale survey of variable stars in the cores of galactic globular clusters using modest instruments.

ACKNOWLEDGMENTS

We thank C. Alard for helpful advice on the use of ISIS 2.1, and appreciate R. Barbera's help in providing us with his AVE program. We also thank George Wendt for the use of his period analysis software. We are grateful to H. Smith for several useful comments on the manuscript.

REFERENCES

Alard, C. and Lupton, R., 1998, *ApJ*, 503, 325
 Alard, C., 2000, *A&AS*, 144, 363
 Bailey, S., 1913, *Obs.*, 78, 1
 Bakos, G., Benko, J., Juresik, J., 2000, *AcA*, 50, 221 (B00)
 Blahzko, S., 1907, *Astron. Nachr.* 175, 325
 Carretta, E., Cacciari, C., Ferraro, F., Pecci, F., Tessicini, G., 1998, *MNRAS*, 298, 1005 (C98)
 Clement, C., Muzzin, A., Dufton, T., Ponnampalam, J., Wang, J., Burford, A., Richardson, T., Rosebery, J., Sawyer, H., 2001, *AJ*, 122, 2587 (C01)
 Corwin, M., Carney, B., 2001, *AJ*, 122, 3183 (CC01)
 Corwin, M., Carney, B., Allen, D., 1999, *AJ*, 117, 1332
 Evstigneeva, N., Samus', N., Tsvetkova, T., Shokin, Y., 1994 *Pisma Astron. Zh.*, 20, 693
 Guhathakurta, P., Yanny, B., Bahcall, J., Schneider, D., 1994, *AJ*, 108, 1786
 Kholopov, P., 1977, *Perem. Zvezdy*, 20, 313
 Oosterhoff, P., 1939, *Obs.*, 62, 104
 Sawyer Hogg, H., 1973, *P.D.D.O.*, 3, 1
 Scargle, J., 1982, *ApJ*, 263, 835
 Stellingwerf, R., 1978, *ApJ*, 224, 953

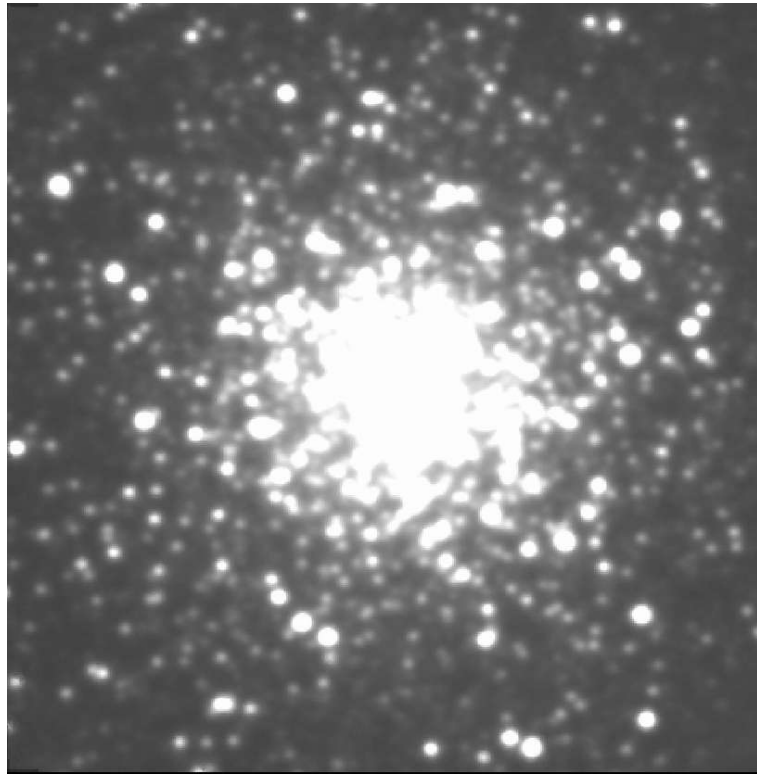


Figure 1. The ISM reference image, which is a composite of images taken between March and May, 2001.

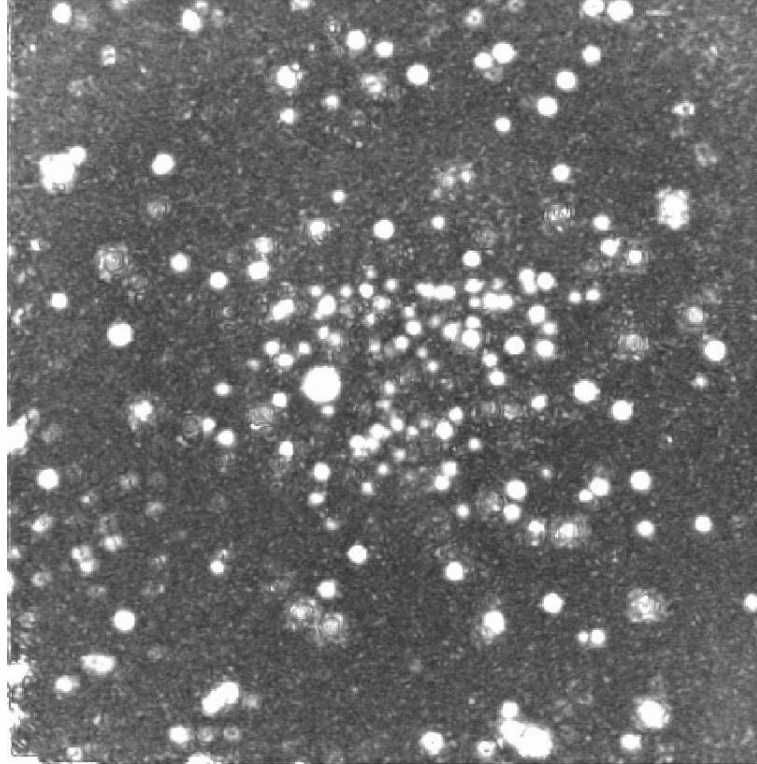


Figure 2. The *var.fits* file from the ISM routine. This is the clipped median image of the normalized residual images. The radius of the residual object scales with the variability of the associated star.

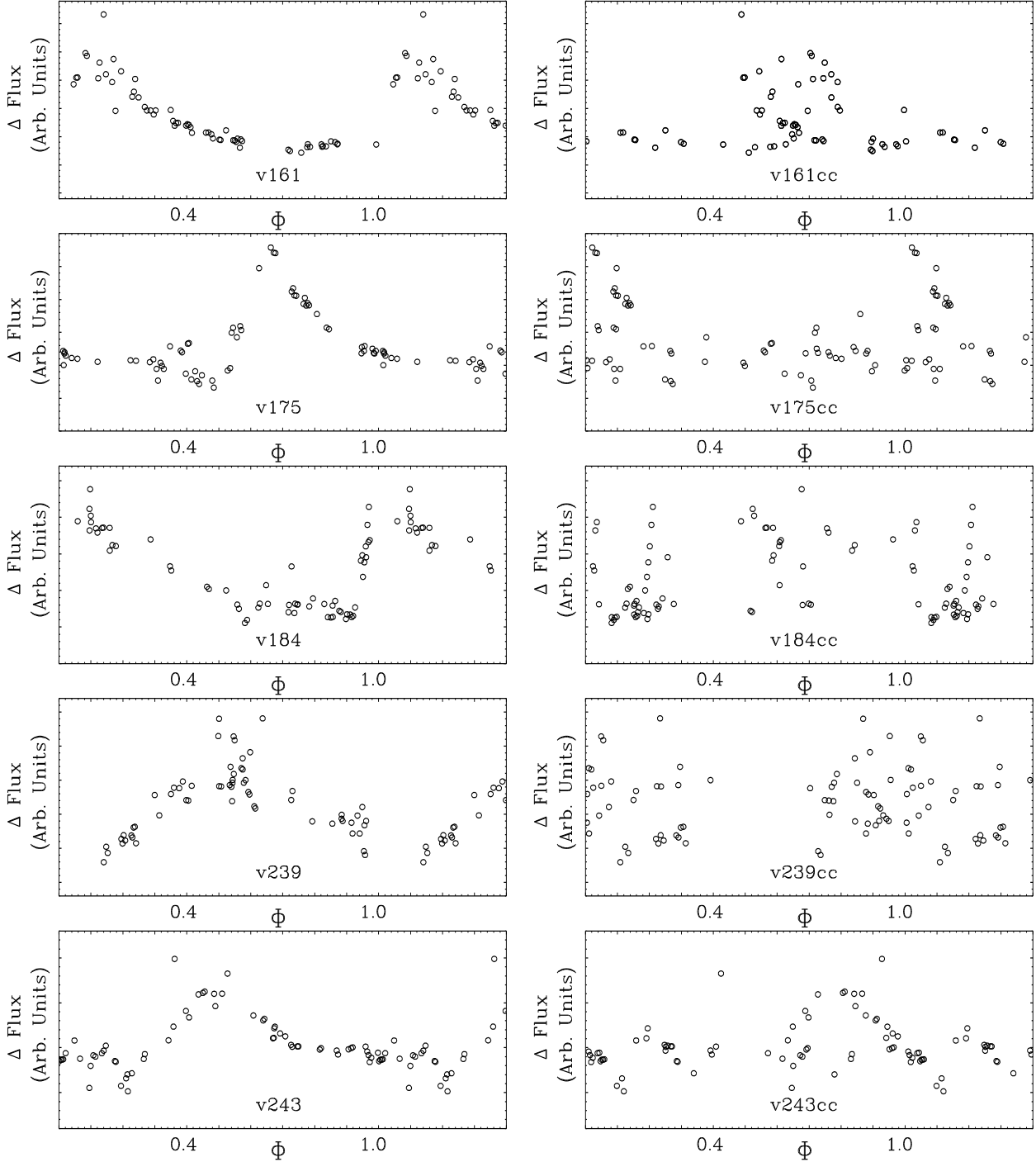


Figure 3. Comparison light curves for five stars with disputed periods, as discussed in §4.1.2. Light curves on the left are phased using the periods obtained through the PDMP analysis of our data. Light curves on the right plot the same data using the CC01 periods.

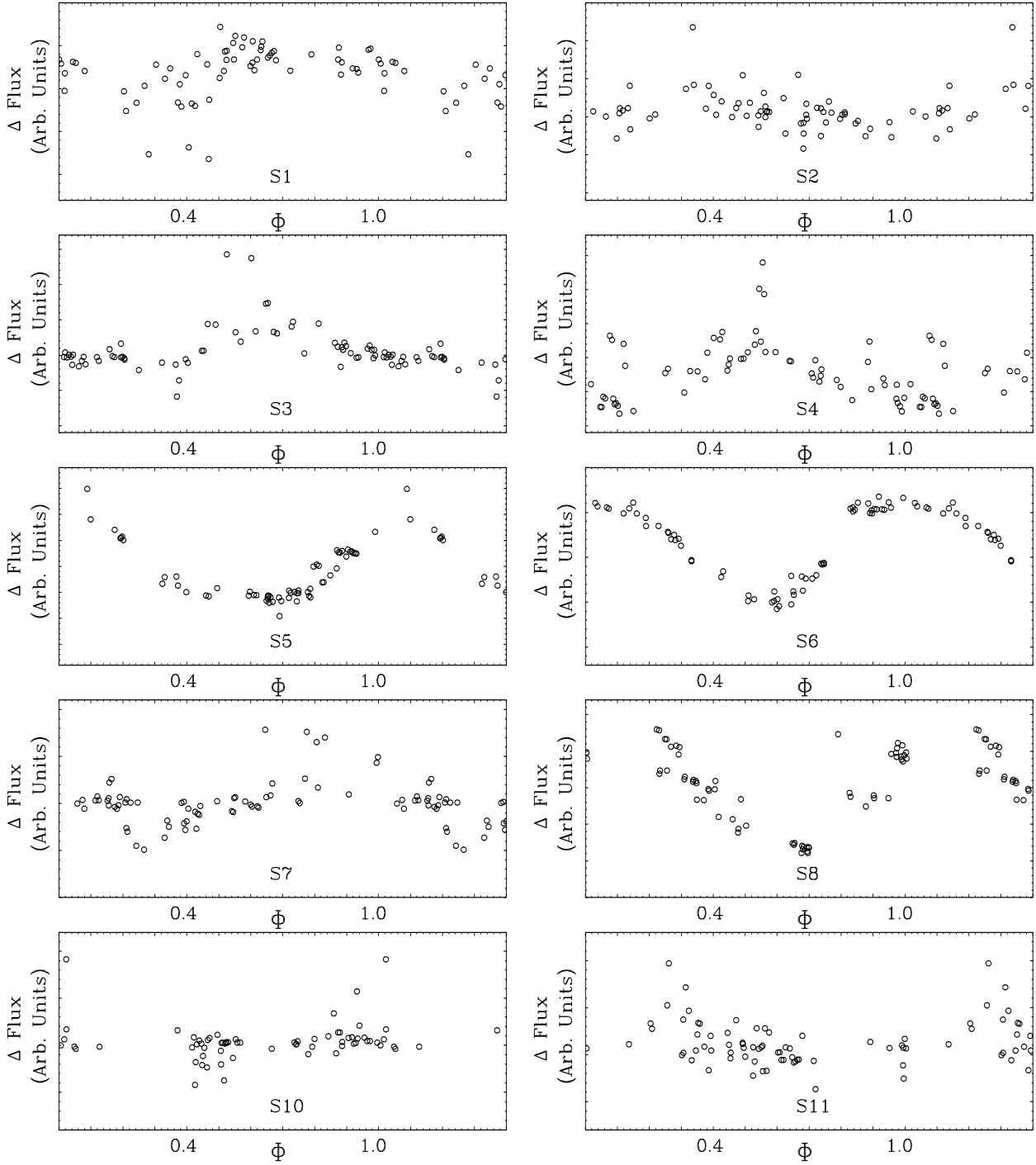


Figure 4. Light curves for each of the newly discovered variable stars for which periods could be determined. (Table 1)

Table 1. Data for variable stars in the core of M3.

ID ^a	Type ^b	$\alpha(sec)$ ^c	$\delta(')$ ^c	Period ^d	Period (Pub.) ^e	Comment ^f
v3	RR0	13:42:15.7	28:21:41.4	0.5582	0.5582	
v4	RR0	13:42:08.2	28:22:33.5	0.5849		n
v7	RR0	13:42:11.1	28:24:10.4	0.4974	0.4974	pc
v8	RR0	13:42:05.3	28:22:18.7	0.6371	0.6392	
v27	RR0	13:42:03.2	28:20:59.2	0.5790	0.5791	n
v28	RR0	13:42:09.6	28:20:56.5	0.4706	0.4699	n
v29	RR0	13:42:06.6	28:21:28.6	0.4715	0.4711	t
v30	RR0	13:42:08.8	28:23:40.1	0.5122	0.5121	
v31	RR0	13:42:14.0	28:23:47.6	0.5807	0.5807	
v32	RR0	13:42:12.4	28:23:42.5	0.4954	0.4954	pc
v33	RR0	13:42:16.8	28:21:13.6	0.5252	0.5252	n
v41	RR0	13:42:04.5	28:23:36.0	0.4854	0.4866	t
v42	RR0	13:42:05.6	28:23:22.5	0.5901	0.5901	
v43	RR0	13:42:19.1	28:23:07.2	0.5406	0.5405	
v58	RR0	13:42:05.0	28:23:28.2	0.5171	0.5171	
v76	RR0	13:42:10.4	28:21:14.1	0.5018	0.5018	n
v77	RR0	13:42:04.4	28:23:09.8	0.4594	0.4594	t
v78	RR0	13:42:15.1	28:23:48.7	0.6120	0.6120	
v87	RR01	13:42:19.8	28:23:42.6	0.3575	0.3575	
v88	RR1	13:42:08.9	28:21:32.4	0.2988	0.2985	n, pc
v89	RR0	13:42:13.6	28:20:51.7	0.5485	0.5485	
v101	RR0	13:42:15.0	28:24:05.8	0.6439	0.6439	n, pc
v109	RR0	13:42:04.8	28:22:44.6	0.5339	0.5339	n
v110	RR0	13:42:04.0	28:22:26.7	0.5355	0.5355	n
v111	RR0	13:42:04.5	28:23:04.0	0.5104	0.5102	
v121	RR0	13:42:08.2	28:23:37.7	0.5352	0.5352	
v122	RR0	13:42:09.1	28:21:55.5	0.5165	0.5060	m(v229), n, t
v129	RR1	13:42:08.3	28:23:59.6	0.4056	0.4061	
v131	RR1	13:42:06.0	28:23:09.3	0.2977	0.2977	
v132	RR1	13:42:07.5	28:22:19.9	0.3398	0.3399	
v133	RR0	13:42:07.1	28:23:26.1	0.5508	0.5507	
v134	RR0	13:42:09.8	28:23:34.9	0.6181	0.6181	n
v135	RR0	13:42:09.5	28:23:20.7	0.5684	0.5684	n
v136	RR0	13:42:09.6	28:23:16.1	0.6173	0.6172	
v137	RR0	13:42:15.5	28:22:23.3	0.5752	0.5752	
v139	RR0	13:42:14.1	28:23:10.6	0.5601	0.5600	
v142	RR0	13:42:09.3	28:21:43.9	0.5687	0.5686	pc
v143	RR0	13:42:08.9	28:22:59.1	0.5965	0.5965	
v144	RR0	13:42:15.6	28:21:02.7	0.5968	0.5968	
v145	RR0	13:42:13.6	28:22:51.1	0.5145	0.5145	n
v146	RR0	13:42:18.5	28:21:44.2	0.5967	0.5967	n
v147	RR1	13:42:09.9	28:23:29.5	0.3465	0.3465	
v148	RR0	13:42:11.0	28:23:20.1	0.4673	0.4660	t
v149	RR0	13:42:14.1	28:23:35.4	0.5482	0.5500	pc, t
v150	RR0	13:42:16.7	28:23:20.6	0.5240	0.5239	
v151	RR0	13:42:10.0	28:22:01.6	0.5170	0.5178	
v152	RR1	13:42:17.5	28:23:33.7	0.3261	0.3261	
v154	W Vir	13:42:11.7	28:22:13.9	15.23	15.28	t
v156	RR0	13:42:12.0	28:22:01.1	0.5320	0.5320	
v157	RR0	13:42:10.2	28:23:18.1	0.5427	0.5419	
v159	RR0	13:42:10.4	28:22:58.9	0.5337	0.5337	n
v161	RR0	13:42:12.8	28:21:45.1	0.5264	0.5144	pc, t
v165	RR0	13:42:17.1	28:23:03.1	0.4836	0.4850	t
v166	RR01	13:42:04.2	28:22:34.8	0.4852	0.4852	
v167	RR0	13:42:05.6	28:22:05.7	0.6440	0.6440	n
v168	RR1	13:42:08.1	28:22:49.6	0.2760	0.2764	
v170	RR1	13:42:09.4	28:23:15.5	0.4324	0.4357	t
v171	RR0	13:42:09.5	28:22:59.4	0.3032	0.3038	
v172	RR0	13:42:09.9	28:23:08.4	0.5423	0.5423	n
v173	RR0	13:42:10.6	28:23:21.6	0.6070	0.6070	

Table 1 – *continued*

ID ^a	Type ^b	$\alpha(sec)$ ^c	$\delta(')$ ^c	Period ^d	Period (Pub.) ^e	Comment ^f
v174	RR0	13:42:10.9	28:22:08.7	0.5945	0.5945	n, pc
v175	RR0	13:42:14.6	28:23:09.2	0.5698	0.5658	n, t
v176	RR0	13:42:15.0	28:23:16.0	0.5399	0.5406	n, pc
v177	RR1	13:42:16.3	28:22:13.8	0.3481	0.3487	n
v178	RR1	13:42:17.5	28:23:29.7	0.2670	0.2674	t
v184	RR0	13:42:09.6	28:22:27.6	0.5313	0.5296	
v186	RR0	13:42:12.5	28:21:39.5	0.6633	0.6633	n
v187	RR0	13:42:09.7	28:22:51.9	0.4649	0.5841	n
v188	RR1	13:42:09.6	28:23:06.5	0.2663	0.2663	
v189	RR0	13:42:09.6	28:22:21.7	0.6129	0.6187	
v190	RR0	13:42:10.9	28:23:11.1	0.5228	0.5228	n
v191	RR0	13:42:11.6	28:23:06.0	0.5193	0.5192	n
v192	RR0	13:42:11.4	28:22:46.8	0.4972	0.4815	
v193	RR0	13:42:12.6	28:22:35.7	0.7477	0.7328	pc, t
v194	RR0	13:42:12.8	28:22:29.8	0.4890	0.4892	n, pc
v195	RR0	13:42:10.5	28:22:14.6	0.6448	0.6439	n
v197	RR0	13:42:15.9	28:22:52.1	0.4999	0.4999	pc
v200	RR0	13:42:11.2	28:23:03.9	0.5292		n, pc
v201	RR0	13:42:11.8	28:22:33.9	0.5407	0.5396	t
v207	RR1	13:42:14.2	28:22:11.4	0.4291	0.3449	pc
v208	RR1	13:42:11.7	28:21:44.4	0.3384	0.3373	n, t
v209	RR1	13:42:06.4	28:21:02.7	0.3483	0.3472	t
v212	RR0	13:42:09.9	28:22:04.3	0.5422	0.5422	n
v213	RR1	13:42:09.6	28:22:12.5	0.2994	0.2997	n, pc
v214	RR0	13:42:13.9	28:22:48.6	0.5395	0.5395	n, t
v215	RR0	13:42:10.5	28:22:41.5	0.5331	0.5331	n
v216	RR1	13:42:13.6	28:22:31.4	0.3465	0.3465	
v218	RR0	13:42:13.6	28:22:13.0	0.5440	0.5431	n
v219	RR0	13:42:07.1	28:22:57.9	0.6138	0.6114	n, t
v220	RR0	13:42:14.0	28:22:26.8	0.5999	0.5959	pc
v221	RR0	13:42:10.2	28:22:28.8	0.6098	0.3787	pc
v222	RR0	13:42:18.8	28:21:39.0	0.5007	0.5007	n
v223	RR1	13:42:13.3	28:22:36.4	0.3293	0.3296	
v224		13:42:09.6	28:22:46.4			nv
v226	RR0	13:42:13.0	28:22:24.0	0.4887	0.4877	n, t
v229	RR0	13:42:09.9	28:23:04.5	0.6877		m(v122), n, t
v234	RR0	13:42:13.1	28:22:02.7	0.5495		n, pc
v235	RR0	13:42:13.8	28:23:19.6	0.7594	0.7617	n, pc, t
v239	RR0	13:42:09.9	28:22:32.1	0.6766	0.3334	n, t
v240	RR0	13:42:09.5	28:22:35.1	0.2760	0.2765	
v241	RR0	13:42:09.7	28:22:50.3	0.5450	0.5962	m(v262), n, t
v242	RR0	13:42:13.2	28:22:24.3	0.6513		n
v243	RR0	13:42:12.3	28:22:15.5	0.6351	0.6322	n, t
v245	RR1	13:42:09.9	28:22:59.8	0.2840		
v246	RR1	13:42:12.8	28:22:40.5	0.3392	0.3384	n
v250	RR0	13:42:10.6	28:22:52.4	0.5586		m, n, t
v253	RR1	13:42:12.2	28:22:32.7	0.3328		n, pc
v254	RR0	13:42:12.4	28:22:53.2	0.6056		
v256	RR1	13:42:13.1	28:22:58.5	0.3181	0.3156	n
v257	RR0	13:42:13.0	28:22:28.1	0.6019		n
v258	RR0	13:42:14.3	28:23:31.0	0.7134	0.7134	n
v259	RR0	13:42:14.6	28:22:54.7	0.5009	0.3335	n, pc
v261	RR0	13:42:10.1	28:22:40.2	0.4447	0.4447	
v262	RR0	13:42:10.8	28:22:37.8	0.5647		m(v241), n, t
v264	RR1	13:42:10.9	28:22:29.7	0.3563		n
v270	RR0	13:42:12.0	28:23:31.8	0.4938	0.6903	n, pc
v271	RR0	13:42:12.2	28:23:17.8	0.6329	0.6327	n
v273	lp	13:42:06.8	28:20:56.8	46.43		pc, t

Table 1 – *continued*

ID ^a	Type ^b	$\alpha(sec)$ ^c	$\delta(')$ ^c	Period ^d	Period (Pub.) ^e	Comment ^f
S1	RR1	13:42:06.5	28:20:59.2	0.3868		n, t
S2	RR1	13:42:17.7	28:21:06.2	0.2980		n, t
S3	RR0	13:42:10.8	28:21:59.2	0.3965		n, t
S4	RR0	13:42:11.1	28:22:02.4	0.5162		n
S5	RR1	13:42:04.7	28:22:05.1	0.5075		t
S6	RR1	13:42:09.9	28:22:15.7	0.3483		pc
S7	RR0	13:42:10.7	28:22:17.9	0.6090		n, t
S8	W Vir	13:42:12.8	28:22:49.6	1.3270		t
S9	lp	13:42:10.7	28:22:58.1			pc, t, v
S10	RR0	13:42:04.9	28:22:06.0	0.4261		n, pc, t
S11	RR0	13:42:08.0	28:23:26.8	0.4778		n, t
S12	RR0	13:42:08.0	28:23:23.7			t, v

^aIdentification taken from C01 and B00. New (or suspected new) variables are assigned names S1, S2, etc. Only the primary period is given for RR01 stars.

^bType ‘lp’ refers to long period variables of undetermined class.

^cCoordinates taken from our mapping using B00 data, as described in Sec. 3.2. Values are generally within 0.1 arcsec of B00.

^dPeriod found by our analysis, given to four decimal places.

^eAll periods are from CC01, with the exception of v154 & v166, which are from C01, and v270 & v271, which are from B00. Periods are rounded to four decimal places for comparison.

^fAdditional information about the star: pc—poor coverage of light curve; m—merged with another star; n—significant scatter in light curve; nv—star does not appear to be variable; t—additional discussion of star in the main text; v—variable, but no clear period.